Probing spatial orientability of a Friedmann-Robertson-Walker spatially flat spacetime

N. A. Lemos,[1,*] D. Müller,[2,†] and M. J. Rebouças[3,‡]

[1]*Instituto de Física, Universidade Federal Fluminense, Av. Litorânea, S/N 24210-340 Niterói RJ, Brazil*
[2]*Instituto de Física, Universidade de Brasília, 70919-970 Brasília DF, Brazil*
[3]*Centro Brasileiro de Pesquisas Físicas, Rua Dr. Xavier Sigaud 150, 22290-180 Rio de Janeiro RJ, Brazil*

(Received 4 March 2022; accepted 8 July 2022; published 27 July 2022)

One important global topological property of a spacetime manifold is orientability. It is widely believed that spatial orientability can only be tested by global journeys around the Universe to check for orientation-reversing closed paths. Since such global journeys are not feasible, theoretical arguments that combine universality of physical experiments with local arrow of time, *CP* violation and *CPT* invariance are usually offered to support the choosing of time- and space-orientable spacetime manifolds. The nonexistence of globally defined spinor fields on a nonorientable spacetime is another theoretical argument for orientability. However, it is conceivable that orientability can be put to test by local physical effects. In this paper, we show that it is possible to locally access spatial orientability of a spatially flat Friedmann-Robertson-Walker spacetime through quantum vacuum electromagnestic fluctuations. We argue that a putative nonorientability of the spatial sections of spatially flat Friedmann-Robertson-Walker spacetime can be ascertained by the study of the stochastic motions of a charged particle or a point electric dipole under quantum vacuum electromagnetic fluctuations. In particular, the stochastic motions of a dipole permit the recognition of a presumed nonorientability of three space in itself.

DOI: 10.1103/PhysRevD.106.023528

I. INTRODUCTION

The standard approach to model the Universe starts with two basic assumptions. First, Weyl's principle [1,2] is postulated, which entails[1] the existence of a cosmic time t. Second, it is assumed that our three-dimensional space is homogeneous and isotropic (cosmological principle). The most general spacetime geometry that embodies these assumptions is the Friedmann-Robertson-Walker (FRW) metric

$$ds^2 = c^2dt^2 - a^2(t)\left[\frac{dr^2}{1-kr^2} + r^2(d\theta^2 + \sin^2\theta d\phi^2)\right], \quad (1)$$

where c is the speed of light, $a(t)$ is the scale factor, and the spatial curvature is specified by the constant k, which takes the values $k = 0, \pm 1$ for Euclidean, spherical and hyperbolic geometries, respectively.

The metric (1) expresses locally the two above basic assumptions. It does not specify the topology of the spacetime manifold $\mathcal{M}_4$ or of the corresponding spatial ($t = \text{const}$) section M_3. However, the FRW metric (1) is consistent with the global decomposition $\mathcal{M}_4 = \mathbb{R} \times M_3$, which we assume in this work.

Regarding the spatial geometry, recent high precision cosmic microwave background radiation [CMB(R)] data from the Planck satellite [6,7] have provided strong evidence that the Universe is very nearly flat with curvature parameter $|\Omega_k| < 0.003$, which is compatible with the standard inflationary predictions that the spatial curvature should be very small today. These indications support the assumption we make in this work that the spatial section M_3 is flat ($k = 0$).

As to the topology of the spatial sections, we first note that the FRW geometry (1) constrains but does not specify the topology of M_3. In this way, no classical geometric theory as, for example, general relativity can be used to derive the M_3 topology. However, for $k = 0$, it is a mathematical fact that, in addition to the simply connected Euclidean space $\mathbb{E}^3$, there are 17 topologically inequivalent quotient flat manifolds with nontrivial topology [8,9]. Given this set of topological possibilities for M_3 and despite our present-day inability to infer the topology from

*nivaldolemos@id.uff.br
†dmuller@unb.br
‡reboucas.marcelo@gmail.com

[1]We adopt here a formulation of Weyl's principle in which it is assumed that world lines of fundamental particles (galaxies, galaxy clusters) form, on average, a congruence of nonintersecting diverging geodesics emerging from the distant past and orthogonal to space-like hypersurfaces M_3. In this form the principle permits a comoving frame relative to which the constituents of the Universe are at rest on average [3–5].

a fundamental theory, as for example quantum gravity [10], to disclose the spatial topology of FRW spacetime we must rely ultimately on cosmological observations (see the review articles [11–16]) or on local physical experiments.[2]

Topological properties precede the geometrical features of a manifold. Thus, it is important to find out whether, how, and to what extent physical results depend on a nontrivial topology.

Nonstandard choices of the background spatial topology affect the mean squared velocity of charged test particles under quantum vacuum fluctuations of the electromagnetic field. In fact, on the assumption that the net role played by the spatial topology is more clearly ascertained in the static FRW flat spacetime, the question of how a nontrivial topology of the spatial section of Minkowski spacetime modifies the stochastic motions of a test charged particle and a point electric dipole under quantum vacuum fluctuations of the electromagnetic field was studied in recent papers [24,25]. By the way, we mention that the case of a point particle coupled to a massless field living in a topologically nontrivial space was considered in Ref. [26].

Orientability is an important topological property of spacetime manifolds. It is generally assumed that, being a global property, the orientability of three space cannot be tested locally. So, a test for spatial orientability would require a global trip along some specific closed paths around the whole three space to check whether one returns with left- and right-hand sides exchanged. Since such a global expedition does not seem to be feasible at the cosmological scale, theoretical arguments that combine universality of physical experiments with local arrow of time, CP violation and CPT invariance are usually invoked [27–30] to support the choosing of time- and space-orientable manifolds, although there are dissenting stances [31,32]. The impossibility of having globally defined spinor fields on nonorientable spacetime manifolds [33,34] is another theoretical argument to support the choice of space-and-time orientable manifolds.[3]

Since 8 out of the 17 possible flat three-manifolds, M_3, with nontrivial topology are nonorientable [8], the question as to whether velocity fluctuations could be also employed to locally reveal specific topological properties such as orientability was examined in Ref. [25]. It was shown that it is possible to locally access the spatial orientability of Minkowski spacetime through the study of the stochastic motions of a charged particle and a point electric dipole subject to these fluctuations in Minkowski spacetime with orientable and nonorientable spatial topologies. It was found that a characteristic inversion pattern exhibited by certain statistical orientability indicator curves, constructed from the mean square velocity of an electric dipole, can be used as a local physical signature of nonorientability of the spatial section M_3 of Minkowski spacetime.

Thus, a question that naturally arises is how these results are modified in an expanding FRW universe whose curvature parameter is within the bounds determined by Planck data [6,17], which indicate that a flat geometry is a good approximation to model the spatial section of the Universe in the framework of general relativity. To tackle this question, in this paper we study the stochastic motions of a charged particle and a point electric dipole under quantum vacuum electromagnetic fluctuations in a spatially flat FRW geometry with spatial sections endowed with an orientable and its counterpart nonorientable spatial topologies. In so doing we extend the results of [24,25] from the static Minkowski spacetime to a dynamical FRW spacetime. Our result for the orientability indicator is very general, in the sense that it does not depend on the underlying gravitational theory, because it is obtained from first topological-geometrical principles alone.

The structure of the paper is as follows. In Secs. II and III we describe the topological and dynamical settings, respectively. In Secs. IV and V we derive statistical orientability indicators both for the charged particle and the point electric dipole that are independent of any specific metrical theory of gravity. To concretely study the time evolution of the orientability indicators, in Sec. VI we choose general relativity and a barotropic perfect fluid as the matter content. In the case of a charged particle, we show that it is possible to distinguish the orientable from the nonorientable topology by comparing the time evolution of an orientability indicator, defined from the stochastic motion of the particle, in the orientable and nonorientable topologies.

We then turn to the more substantial problem of finding a way to decide about the orientability of a given spatial manifold in itself, without having to compare the results for a nonorientable space with those for its orientable counterpart. Motivated by a dipole's directional properties, we inquire whether the stochastic motions of a point electric dipole would be more effective to unveil the presumed nonorientability of a three space in itself. From the orientability indicators computed for the dipole we identify a characteristic inversion pattern displayed by the orientability indicator curves for the nonorientable topology, implying that the putative nonorientability can be detected *per se*.

In Sec. VII we present our final remarks and summarize our findings, which indicate that it may be possible to locally disclose a conceivable spatial nonorientability of FRW spacetime through the stochastic motions of pointlike "charged" objects under quantum vacuum fluctuations of the electromagnetic field.

[2]For recent constraints on cosmic topology from CMBR data we refer the readers to Refs. [6,17–22]. For some limits on the circles-in-the-sky method designed for the searches of spatial topology through CMBR, see Ref. [23].

[3]One can certainly take advantage of theoretical arguments of this sort to support such underlying assumptions, but not as a replacement to experimental and observational evidence in physics.

II. TOPOLOGICAL FUNDAMENTALS

To make this work to a certain extent self-contained, in this section we define the notation, give some basic definitions and present a few results concerning the topology of flat three-dimensional manifolds that are used in this paper.

We begin by recalling that in the standard cosmological model the spacetime is a manifold $\mathcal{M}_4$ locally endowed with a FRW metric (1) and globally decomposable as $\mathcal{M}_4 = \mathbb{R} \times M_3$. Although the spatial section M_3, whose geometry we assume to be Euclidean, is usually taken to be the simply connected Euclidean space $\mathbb{E}^3$, it can likewise be one of the possible 17 topologically inequivalent multiply connected quotient manifolds $\mathbb{E}^3/\Gamma$ where Γ is a discrete group of isometries or holonomies acting freely on the covering manifold $\mathbb{E}^3$ [8,9]. The quotient manifolds are compact in at least one direction. The action of Γ tiles the noncompact covering space $\mathbb{E}^3$ into infinitely many identical copies of the fundamental domain (FD) or cell (FC). Thus, the multiple connectedness of the quotient manifold gives rise to periodic boundary conditions (repeated domains or cells) on the covering manifold $\mathbb{E}^3$ that are determined by the action of the group Γ on $\mathbb{E}^3$.

An example of flat quotient manifold is the so-called slab space, denoted in the literature by E_{16}, which is open (noncompact) in two independent directions and decomposed into $E_{16} = \mathbb{R}^2 \times \mathbb{S}^1 = \mathbb{E}^3/\Gamma$, where $\mathbb{R}^2$ and $\mathbb{S}^1$ stand for the real plane and the circle, respectively. A fundamental domain is a slab with a pair of opposite faces (two infinite parallel planes) identified through translations. The simply connected covering space $\mathbb{E}^3$ is tiled with these equidistant parallel planes, which together with two noncompact independent spatial directions form the FD of E_{16}. The periodicity in the compact direction is given by the circle $\mathbb{S}^1$, whereas the noncompact independent directions form $\mathbb{R}^2$.

In forming the quotient manifolds M_3 an essential point is that they are obtained from the covering manifold $\mathbb{E}^3$ through identification of points that are equivalent under the action of the group Γ. In this way, each point in the quotient manifold M_3 represents all the equivalent points in the covering space. Thus, for example, for E_{16} quotient space, taking the x direction as compact, one has that, for $n_x \in \mathbb{Z}$ and compact length $L > 0$, points (x, y, z) and $(x + n_x L, y, z)$ are identified. In terms of the covering isometry $\gamma \in \Gamma$ one has

$$P = (x, y, z) \mapsto P' = \gamma P = (x + n_x L, y, z). \quad (2)$$

Another example that we shall be concerned with in this paper is the slab space with flip E_{17}, which involves an additional inversion in a direction orthogonal to the compact direction, that is, one direction in the tiling planes is flipped as one moves from one plane to the next. Taking the x direction as compact and letting the flip be in the y direction, in the covering space $\mathbb{E}^3$ one has

$$P = (x, y, z) \mapsto P' = \gamma P = (x + n_x L, (-1)^{n_x} y, z), \quad (3)$$

and the identification $P \equiv P'$ defines the E_{17} topology.

It should be noted that for each of the 17 quotient manifolds, $\mathbb{E}^3/\Gamma$, the associated periodic conditions on the covering space $\mathbb{E}^3$ are determined by the group Γ, and clearly different discrete isometry groups Γ define different topologies for M_3, which in turn give rise to different periodicities and associated tiling of the covering space $\mathbb{E}^3$.

Unlike the local geometric concept of homogeneity, which is formulated in terms of the action of the local group of isometries, in topological spaces we have the concept of global or topological homogeneity. A way to describe global topological homogeneity of the quotient manifolds is through distance functions. In fact, for any $\mathbf{x} \in M_3$ the distance function $\ell_\gamma(\mathbf{x})$ for a given isometry $\gamma \in \Gamma$ is defined by

$$\ell_\gamma(\mathbf{x}) = d(\mathbf{x}, \gamma\mathbf{x}), \quad (4)$$

where d is the Euclidean metric. The distance function gives the length of the closed geodesic that passes through $\mathbf{x}$ and is associated with a holonomy $\gamma \in \Gamma$. For a globally homogeneous manifold, endowed with a topology defined by a group Γ, the distance function for any covering isometry $\gamma \in \Gamma$ is constant. In globally inhomogeneous manifolds, i.e., manifolds with inhomogeneous topologies, in contrast, the length of the closed geodesic associated with at least one γ is nontranslational (screw motion or flip, for example) and the corresponding distance depends on the point $\mathbf{x} \in M_3$, and then is not constant. In this way, the slab space E_{16} is globally homogeneous since all γs are translations, whereas the slab space with flip, E_{17}, is globally inhomogeneous since the covering group Γ contains a flip, which clearly is a nontranslational holonomy.

Another very important global (topological) property of manifolds that we shall deal with in this paper is orientability, which measures whether one can consistently choose a definite orientation for loops in a manifold. An orientation-reversing path in a manifold M_3 is a path that brings a traveler back to the starting point mirror reversed. Manifolds that contain an orientation-reversing path are nonorientable, whereas those that do not have any such reversing path are called orientable [35]. In two dimensions, one has planes, cylinders, and two tori as examples of orientable surfaces, whereas the Möbius strip and Klein bottle are nonorientable surfaces. For three-dimensional quotient manifolds, when the covering group Γ contains at least one holonomy γ that is a reflection (flip), the associated quotient manifold is nonorientable. In this way, the slab space, E_{16}, is orientable while the slab space with flip, E_{17}, is nonorientable. Clearly nonorientable manifolds are necessarily topologically inhomogeneous as the covering group Γ contains a reflexion, which is a nontranslational covering holonomy.

TABLE I. Names and symbols of two Euclidean orientable and nonorientable quotient manifolds $M_3 = \mathbb{E}^3/\Gamma$ together with the number of compact dimensions (Comp.), orientability and global (topological) homogeneity.

Name	Symbol	Compact Dim.	Orientable	Homogeneous
Slab space	E_{16}	1	Yes	Yes
Slab space with flip	E_{17}	1	No	No

In Table I we collect the names and symbols used to refer to the manifolds together with the number of compact independent dimensions and information concerning their orientability and global homogeneity. In the next section we shall study the motions of a charged test particle and a point electric dipole under quantum vacuum fluctuations of the electromagnetic field in the expanding FRW spacetime whose spatial sections are the manifolds given in Table I.

Finally, we briefly mention a few results that are used throughout this paper (for a detailed discussion we refer the reader to Ref. [30]). All simply connected spacetime manifolds are both time and space orientable. The product of two manifolds is simply connected if and only if the factors are. If the spacetime is of the form $\mathcal{M}_4 = \mathbb{R} \times M_3$ then space orientability of the spacetime reduces to orientability of the three space M_3. This applies to the spacetime endowed both with the E_{16} (orientable) and the E_{17} (nonorientable) topology that we deal with in this paper.

III. NONORIENTABILITY FROM ELECTROMAGNETIC FLUCTUATIONS

As shown in [24,25], nontrivial spatial topologies influence the stochastic motions both of a charged particle and a point electric dipole in the presence of quantum vacuum fluctuations of the electromagnetic field in Minkowski spacetime. Here we investigate how these results are modified if instead of static Minkowski spacetime an expanding FRW flat universe is the background geometry for the motions of the charged particle and the dipole. To this end we consider a spatially flat FRW spacetime endowed with two inequivalent spatial topologies given in Table I, namely the orientable slab space (E_{16}) and the nonorientable slab space with flip (E_{17}).

A. The point charge case

We first consider a nonrelativistic test particle with charge q and mass m locally subjected to vacuum fluctuations of the electric field $\mathbf{E}(\mathbf{x}, t)$ in the topologically nontrivial spacetime manifold equipped with the spatially flat FRW metric

$$ds^2 = dt^2 - a^2(t)(dx^2 + dy^2 + dz^2), \tag{5}$$

which is the particular case of Eq. (1) with $k = 0$ and Cartesian instead of spherical coordinates. The covariant equation of motion is [36]

$$\frac{Du^\mu}{d\tau} \overset{\text{def}}{=} \frac{du^\mu}{d\tau} + \Gamma^\mu_{\alpha\beta} u^\alpha u^\beta = \frac{f^\mu}{m}, \tag{6}$$

where $u^\mu = dx^\mu/d\tau$ is the particle's four-velocity, m is its mass, τ is its proper time and f^μ is the nongravitational four force acting on it. Since we are interested in the motion of a charged particle in an electromagnetic field, the four force is $f^\mu = qF^{\mu\nu}u_\nu$, where $F^{\mu\nu}$ is the electromagnetic field tensor.

In the nonrelativistic case, in which the particle's proper time is indistinguishable from the cosmic time t, the equation of motion for the point charge becomes [37]

$$\frac{d\mathbf{u}}{dt} + 2\frac{\dot{a}}{a}\mathbf{u} = \frac{q}{m}\mathbf{E}(\mathbf{x}, t), \tag{7}$$

which can be written as

$$\frac{1}{a^2}\frac{d}{dt}(a^2\mathbf{u}) = \frac{q}{m}\mathbf{E}(\mathbf{x}, t), \tag{8}$$

where $\mathbf{E} = (E^1, E^2, E^3)$ with $E^i = F^{i0}$. After integration this yields

$$a^2(t)\mathbf{u}(\mathbf{x}, t) = \frac{q}{m}\int_{t_i}^{t} a^2(t')\mathbf{E}(\mathbf{x}, t')dt', \tag{9}$$

where we have assumed that the particle is initially at rest: $\mathbf{u}(\mathbf{x}, t_i) = 0$. Since proper (physical) distances d at time t are related to coordinate distances r by $d = a(t)r$, the proper (physical) velocity $\mathbf{v}$ is related to the coordinate velocity $\mathbf{u}$ at time t by

$$\mathbf{v}(\mathbf{x}, t) = a(t)\mathbf{u}(\mathbf{x}, t). \tag{10}$$

Therefore, in terms of the physical velocity, Eq. (9) becomes

$$\mathbf{v}(\mathbf{x}, t) = \frac{q}{m}\frac{1}{a(t)}\int_{t_i}^{t} a^2(t')\mathbf{E}(\mathbf{x}, t')dt', \tag{11}$$

from which the one can write the dispersion of each velocity component as[4]

$$\langle \Delta v^i(\mathbf{x}, t)^2 \rangle = \frac{q^2}{m^2 a^2(t)}\int_{t_i}^{t}\int_{t_i}^{t} a^2(t')a^2(t'') \times \langle E^i(\mathbf{x}, t')E^i(\mathbf{x}, t'')\rangle_{\text{FRW}} dt'dt'', \tag{12}$$

[4]By definition, $\langle \Delta v^i(\mathbf{x}, t)^2 \rangle = \langle v^i(\mathbf{x}, t)^2 \rangle - \langle v^i(\mathbf{x}, t) \rangle^2$.

where $i = 1, 2, 3$ for the corresponding directions x, y, z.[5] As in Refs. [25,38], here we assume that $\mathbf{x}$ is constant, meaning that in the timescales of interest the particle's position essentially does not change.

B. Velocity dispersion in terms of conformal time

The Friedmann-Robertson-Walker correlation function that appears in Eq. (12) can be more easily computed in terms of the Minkowski spacetime correlation function by making use of how the electromanetic field changes under a conformal transformation. Indeed, in terms of the conformal time η defined by $dt = a(t)d\eta$ the FRW metric becomes

$$ds^2 = a^2(d\eta^2 - dx^2 - dy^2 - dz^2). \tag{13}$$

In these coordinates the electromagnetic field tensor in FRW spacetime is related to the one in Minkowski spacetime M by [37,39]

$$F^{\mu\nu}(\mathbf{x},\eta)_{\mathrm{FRW}} = a^{-4}F^{\mu\nu}(\mathbf{x},\eta)_M. \tag{14}$$

Taking this equation into account, noting further that the coordinate change $t \to \eta$ implies

$$F^{i0}(\mathbf{x},\eta)_{\mathrm{FRW}} = a^{-1}F^{i0}(\mathbf{x},t)_{\mathrm{FRW}}, \tag{15}$$

and changing the integration variable to η using $dt = ad\eta$, Eq. (12) reduces to

$$\langle \Delta v^i(\mathbf{x},t)^2\rangle = \frac{q^2}{m^2a^2(t)}\int_{\eta_i}^{\eta}\int_{\eta_i}^{\eta}\langle E^i(\mathbf{x},\eta')E^i(\mathbf{x},\eta'')\rangle_M d\eta' d\eta''. \tag{16}$$

Therefore, in order to compute the velocity dispersion all one needs is the correlation function in Minkowski spacetime with the time coordinate replaced by η. The result can be expressed in terms of the cosmic time t as long as the scale factor is known as a function of t or η.

Since the correlation function in Eq. (16) is in Minkowski spacetime M, it depends on the topology of the spatial section as discussed in [24,25]. Then the above result for the velocity dispersion (16) in FRW spacetime depends on the topology of the spatial sections M_3 of the FRW spacetime, whose set of possible nonequivalent topologies is identical to the corresponding set for the spatial section M_3 of Minkowski spacetime M. In the next section we shall use this result to derive the velocity dispersion, and thus explicit expressions for a velocity dispersion orientability indicator for manifolds endowed with nonorientable topology E_{17}, and for its orientable counterpart E_{16}.

[5]For any three-vector $\mathbf{b}$ we write either $\mathbf{b} = (b^1, b^2, b^3)$ or $\mathbf{b} = (b_x, b_y, b_z)$ according to convenience.

IV. ORIENTABILITY INDICATORS FOR E_{17} AND E_{16} SPATIAL TOPOLOGIES

In this section, we compute the orientability indicators for a FRW spacetime with flat spatial sections equipped with the nonorientable E_{17} topology. The corresponding results for spatial sections endowed with E_{16} topology follow from those for E_{17} with no need of additional calculations.

Following Yu and Ford [38], we assume that the electric field $\mathbf{E}$ is a sum of classical $\mathbf{E}_c$ and quantum $\mathbf{E}_q$ parts. Since there are no quantum fluctuations of $\mathbf{E}_c$ and $\langle \mathbf{E}_q\rangle = 0$, the two-point function $\langle E^i(\mathbf{x},\eta')E^i(\mathbf{x},\eta'')\rangle_M$ in Eq. (16) involves only the quantum part of the electric field [38].

It can be shown [40] that locally

$$\langle E^i(\mathbf{x},\eta)E^i(\mathbf{x}',\eta')\rangle = \frac{\partial}{\partial x_i}\frac{\partial}{\partial x'_i}D(\mathbf{x},\eta;\mathbf{x}',\eta') - \frac{\partial}{\partial\eta}\frac{\partial}{\partial\eta'}D(\mathbf{x},\eta;\mathbf{x}',\eta'). \tag{17}$$

The topology of the spatial section M_3 is (globally) taken into account as follows. When M_3 is simply connected the Hadamard function $D(\mathbf{x},\eta;\mathbf{x}',\eta')$ is given by

$$D_0(\mathbf{x},\eta;\mathbf{x}',\eta') = \frac{1}{4\pi^2(\Delta\eta^2 - |\Delta\mathbf{x}|^2)}. \tag{18}$$

The subscript 0 indicates standard Minkowski spacetime M, $\Delta\eta = \eta - \eta'$ and $|\Delta\mathbf{x}| \equiv r$ is the spatial separation for topologically trivial Minkowski spacetime:

$$r^2 = (x - x')^2 + (y - y')^2 + (z - z')^2. \tag{19}$$

However, when Minkowski spacetime in endowed with a topologically nontrivial spatial section, the spatial separation r^2 takes a different form that captures the periodic boundary conditions imposed on the covering space $\mathbb{E}^3$ by the covering group Γ, which characterize the spatial topology. In Table II we collect the spatial separations for the topologically nonhomeomorphic Euclidean spaces we shall address in this paper.[6]

To obtain the correlation function for the electric field that is required to compute the velocity dispersion (16) for slab space with flip E_{17}, we replace in Eq. (17) the Hadamard function $D(\mathbf{x},\eta;\mathbf{x}',\eta')$ by its renormalized version given by [24]

[6]The reader is referred to Refs. [12,41,42] for pictures of the fundamental cells and further properties of all possible three-dimensional Euclidean topologies.

TABLE II. Spatial separation in Hadamard function for the multiply connected flat orientable (E_{16}) and its nonorientable counterpart (E_{17}) quotient Euclidean manifolds. The topological compact length is denoted by L. The numbers n_x are integers and run from $-\infty$ to ∞. For each multiply connected topology, when $n_x = 0$ we recover the spatial separation for the simply connected Euclidean three space.

Spatial topology	Spatial separation r^2 for Hadamard function
E_{16}: Slab space	$(x-x'-n_xL)^2+(y-y')^2+(z-z')^2$
E_{17}: Slab space with flip	$(x-x'-n_xL)^2+(y-(-1)^{n_x}y')^2+(z-z')^2$

$$D_{\rm ren}(\mathbf{x},\eta;\mathbf{x}',\eta') = D(\mathbf{x},\eta;\mathbf{x}',\eta') - D_0(\mathbf{x},\eta;\mathbf{x}',\eta') = \sum_{n_x=-\infty}^{\infty\prime} \frac{1}{4\pi^2(\Delta\eta^2 - r^2)}, \tag{20}$$

where here and in what follows $\sum'$ indicates that the Minkowski contribution term $n_x = 0$ is excluded from the summation, $\Delta\eta = \eta - \eta'$, and the spatial separation r for E_{17} is given in Table II. The term with $n_x = 0$ that would be present in the sum (20) is the Hadamard function $D_0(\mathbf{x},\eta;\mathbf{x}',\eta')$ for Minkowski spacetime with simply connected spatial section $\mathbb{E}^3$. This term has been subtracted out from the sum because it gives rise to an infinite contribution to the velocity dispersion [24,25].

Thus, from Eq. (17) the renormalized correlation functions

$$\langle E^i(\mathbf{x},\eta)E^i(\mathbf{x}',\eta')\rangle_{\rm ren} = \frac{\partial}{\partial x_i}\frac{\partial}{\partial x'_i} D_{\rm ren}(\mathbf{x},\eta;\mathbf{x}',\eta') - \frac{\partial}{\partial\eta}\frac{\partial}{\partial\eta'} D_{\rm ren}(\mathbf{x},\eta;\mathbf{x}',\eta'), \tag{21}$$

where $D_{\rm ren}(\mathbf{x},\eta;\mathbf{x}',\eta')$ depends on the spatial topology through r according to (20) and Table II.

From Eqs. (21) and (20) with r given in Table II the electric field correlation functions for E_{17} topology are found to be given by

$$\langle E_x(\mathbf{x},\eta)E_x(\mathbf{x}',\eta')\rangle^{E_{17}}_{\rm ren} = \sum_{n_x=-\infty}^{\infty\prime} \frac{\Delta\eta^2 + r^2 - 2r_x^2}{\pi^2[\Delta\eta^2 - r^2]^3}, \tag{22}$$

$$\langle E_y(\mathbf{x},\eta)E_y(\mathbf{x}',\eta')\rangle^{E_{17}}_{\rm ren} = \sum_{n_x=-\infty}^{\infty\prime} \left[\frac{(3-(-1)^{n_x})\Delta\eta^2}{2\pi^2[\Delta\eta^2 - r^2]^3} + \frac{(1+(-1)^{n_x})r^2 - 4(-1)^{n_x}r_y^2}{2\pi^2[\Delta\eta^2 - r^2]^3}\right], \tag{23}$$

$$\langle E_z(\mathbf{x},\eta)E_z(\mathbf{x}',\eta')\rangle^{E_{17}}_{\rm ren} = \sum_{n_x=-\infty}^{\infty\prime} \frac{\Delta\eta^2 + r^2 - 2r_z^2}{\pi^2[\Delta\eta^2 - r^2]^3}, \tag{24}$$

where $\Delta\eta = \eta - \eta'$ and

$$r_x = x - x' - n_xL, \qquad r_y = y - (-1)^{n_x}y', \qquad r_z = z - z', \qquad r = \sqrt{r_x^2 + r_y^2 + r_z^2}. \tag{25}$$

The orientability indicator $I^{E_{17}}_{v_i^2}$ that we will consider here is defined by replacing the electric field correlation functions in Eq. (16) by their renormalized counterparts (21) in which r is given in Table II, namely

$$I^{E_{17}}_{v_i^2}(\mathbf{x},t) = \frac{q^2}{m^2a^2(t)}\int_0^\eta\int_0^\eta \langle E^i(\mathbf{x},\eta')E^i(\mathbf{x},\eta'')\rangle^{E_{17}}_{\rm ren} d\eta' d\eta''. \tag{26}$$

Equation (20) makes it is clear that the orientability indicator $I^{E_{17}}_{v_i^2}$ is the difference between the velocity dispersion in E_{17} and the one in Minkowski with trivial (simply connected) topology.

A. Orientability indicator: General definition

For later use and for the sake of generality, some words of clarification are in order at this point before proceeding to the calculation of the components of the statistical indicator. From Eqs. (16) and (20) a definition of the orientability indicator for a general multiply connected flat topology can be written in the form [25]

$$I^{MC}_{v_i^2} = \langle\Delta v_i^2\rangle^{MC} - \langle\Delta v_i^2\rangle^{SC}, \tag{27}$$

where $\langle\Delta v_i^2\rangle$ is the mean square velocity dispersion, and the superscripts MC and SC stand for multiply and simply connected topologies, respectively. The right-hand side of (27) is defined in the following way: one first takes the difference of the two terms with $\mathbf{x}' \neq \mathbf{x}$ and then sets $\mathbf{x}' = \mathbf{x}$. Since $I^{MC}_{v_i^2}$ is not simply the velocity dispersion $\langle\Delta v_i^2\rangle^{MC}$ but the difference (27), the possibility that it takes negative values should not be a matter of worry, a point that does not seem to have been appreciated in some previous works in which this indicator was implicity used [24,38,43–49] together with the particular assumption that the second term vanishes.[7]

At first sight, the indicator (27) does not seem measurable because it involves the difference of quantities associated with two different spacetimes, but spacetime is unique. However, $I^{MC}_{v_i^2}$ is accessible by measurements performed only in our spacetime, which is to be tested

[7]It is experimentally and theoretically unsettled whether the simply connected term on the right-hand side of (27) vanishes or not. We adopt the general view that it is nonzero [25]. It is only under the very special assumption that it vanishes that one stumbles upon the counterintuitive negative values for mean square velocities often found in the literature [24,38,43,44,46–49].

for multiple connectedness, by the following procedure. First one would measure the velocity correlation function $\langle \Delta v_i(\mathbf{x},t)\Delta v_i(\mathbf{x}',t)\rangle^{\exp}$ for $\mathbf{x}\neq\mathbf{x}'$, then one would subtract out the correlation function $\langle \Delta v_i(\mathbf{x},t)\Delta v_i(\mathbf{x}',t)\rangle^{SC}$ that can be theoretically computed for $\mathbf{x}\neq\mathbf{x}'$ for the corresponding topologically trivial (simply connected) FRW spacetime, just as was done in the Appendix of Ref. [25] in the case of the Minkowski spacetime.[8] Finally, the corresponding curve for the difference (27) as a function of time would be plotted in the coincidence limit $\mathbf{x}=\mathbf{x}'$ (see, for example, the figures in Sec. VI). This approach is similar to one used in cosmic crystallography, which is intended to detect cosmic topology from the distribution of discrete cosmic sources [50]. A topological signature of any multiply connected three manifold of constant curvature is given by a constant times the difference $\Phi^{MC}_{\exp}(s_i)-\Phi^{SC}_{\exp}(s_i)$ of the expected pair separation histogram corresponding to the multiply connected manifold and the expected pair separation histogram for the underlying simply connected covering manifold [51,52], whose expression can be derived in analytical form [51,53].

It should be noticed that, although with the present techniques the second term on the right-hand side of (27) cannot be directly computed at $\mathbf{x}=\mathbf{x}'$, we can nonetheless presume that a rigorous theoretical treatment may allow a consistent determination of this term. From our current knowledge of the theory, one can also reasonably expect that a correct renormalization procedure will not significantly change the qualitative features of the two terms, at least not to the extent that it would affect comparison with observational data.

B. Orientability indicators for charged point particle

Let us return to the calculation of the components of the orientability indicator for E_{17} topology. Since the correlation functions (22) to (24) depend on η and η' only through their difference, the changes of integration variables $\eta_1=\eta'-\eta_i$ and $\eta_2=\eta''-\eta_i$ in Eq. (16) allow the components of the velocity dispersion to be computed with the help of the integrals [24]

$$\begin{aligned}\mathcal{I}&=\int_0^{\Delta\eta}\int_0^{\Delta\eta}d\eta_1 d\eta_2\,\frac{1}{[(\eta_2-\eta_1)^2-r^2]^3},\\&=\frac{\Delta\eta}{16r^5(\Delta\eta^2-r^2)}\left\{4r\Delta\eta-3(r^2-\Delta\eta^2)\ln\frac{(r-\Delta\eta)^2}{(r+\Delta\eta)^2}\right\},\end{aligned}\tag{28}$$

and

$$\begin{aligned}\mathcal{J}&=\int_0^{\Delta\eta}\int_0^{\Delta\eta}d\eta_1 d\eta_2\,\frac{(\eta_2-\eta_1)^2}{[(\eta_2-\eta_1)^2-r^2]^3}\\&=\frac{\Delta\eta}{16r^3(\Delta\eta^2-r^2)}\left\{4r\Delta\eta+(r^2-\Delta\eta^2)\ln\frac{(r-\Delta\eta)^2}{(r+\Delta\eta)^2}\right\},\end{aligned}\tag{29}$$

in which $\Delta\eta=\eta-\eta_i$.

Inserting Eqs. (22)–(29) into Eq. (16) and taking the coincidence limit $\mathbf{x}'\to\mathbf{x}$ we find

$$\begin{aligned}I^{E_{17}}_{v_x^2}(\mathbf{x},t)_{\mathrm{FRW}}=\sum_{n_x=-\infty}^{\infty\prime}\frac{q^2\Delta\eta}{16\pi^2m^2r^5(\Delta\eta^2-r^2)a^2(t)}\Big\{&4r\Delta\eta(\bar r_x^2+r^2)\\&+(\Delta\eta^2-r^2)(3\bar r_x^2-r^2)\ln\frac{(r-\Delta\eta)^2}{(r+\Delta\eta)^2}\Big\},\end{aligned}\tag{30}$$

$$\begin{aligned}I^{E_{17}}_{v_y^2}(\mathbf{x},t)_{\mathrm{FRW}}=\sum_{n_x=-\infty}^{\infty\prime}\frac{q^2\Delta\eta}{32\pi^2m^2r^5(\Delta\eta^2-r^2)a^2(t)}\Big\{&4r\Delta\eta(\bar r_y^2+(3-(-1)^{n_x})r^2)\\&+(\Delta\eta^2-r^2)[3\bar r_y^2-(3-(-1)^{n_x})r^2]\ln\frac{(r-\Delta\eta)^2}{(r+\Delta\eta)^2}\Big\},\end{aligned}\tag{31}$$

[8]We do not present here the results for the topologically trivial FRW spacetime for the sake of brevity.

$$I^{E_{17}}_{v_z^2}(\mathbf{x},t)_{\mathrm{FRW}} = \sum_{n_x=-\infty}^{\infty\prime} \frac{q^2\Delta\eta}{16\pi^2 m^2 r^5(\Delta\eta^2-r^2)a^2(t)}\left\{4r\Delta\eta(\bar{r}_z^2+r^2) + (\Delta\eta^2-r^2)(3\bar{r}_z^2-r^2)\ln\frac{(r-\Delta\eta)^2}{(r+\Delta\eta)^2}\right\}, \tag{32}$$

where

$$r = \sqrt{n_x^2L^2 + 2(1-(-1)^{n_x})y^2}, \tag{33}$$

$$\bar{r}_x^2 = r^2 - 2r_x^2 = -n_x^2L^2 + 2(1-(-1)^{n_x})y^2, \tag{34}$$

$$\bar{r}_y^2 = (1+(-1)^{n_x})r^2 - 8(-1)^{n_x}(1-(-1)^{n_x})y^2, \\ = (1+(-1)^{n_x})n_x^2L^2 + 8(1-(-1)^{n_x})y^2, \tag{35}$$

$$\bar{r}_z^2 = r^2 - 2r_z^2 = r^2, \tag{36}$$

with the use of Eq. (25) in the coincidence limit.

Note that the velocity dispersion depends not only on the time interval $\Delta t = t - t_i$ (or $\Delta\eta = \eta - \eta_i$) but also on t (or η) itself. This was to be expected because in a dynamical universe invariance under time translations is lost.

The orientability indicator for E_{16} follows easily from the results for E_{17}. The factors of $(-1)^{n_x}$ that appear in Eqs. (30)–(32) arise from derivatives with respect to y' in the separation r given in Table II. Hence, the results for E_{16} are immediately obtained from those for E_{17} by simply replacing $(-1)^{n_x}$ by 1 everywhere in Eqs. (30)–(32). This leads to

$$I^{E_{16}}_{v_x^2}(\mathbf{x},t)_{\mathrm{FRW}} = -\frac{q^2\Delta\eta}{4\pi^2 m^2 a^2(t)}\sum_{n_x=-\infty}^{\infty\prime}\frac{1}{n^3L^3}\ln\frac{(n_xL-\Delta\eta)^2}{(n_xL+\Delta\eta)^2}, \tag{37}$$

$$I^{E_{16}}_{v_y^2}(\mathbf{x},t)_{\mathrm{FRW}} = I^{E_{16}}_{v_z^2}(\mathbf{x},t)_{\mathrm{FRW}} = \frac{q^2\Delta\eta}{8\pi^2 m^2 a^2(t)}\sum_{n_x=-\infty}^{\infty\prime}\left\{\frac{4\Delta\eta}{n_x^2L^2(\Delta\eta^2-n_x^2L^2)} + \frac{1}{n_x^3L^3}\ln\frac{(n_xL-\Delta\eta)^2}{(n_xL+\Delta\eta)^2}\right\}. \tag{38}$$

V. NONORIENTABILITY WITH POINT ELECTRIC DIPOLE

A noteworthy outcome of the previous section is that the time evolution of the orientability indicator for a charged particle can be used to locally differentiate an orientable (E_{16}) from a nonorientable (E_{17}) spatial section of Minkowski spacetime. However, it cannot be used to decide whether a given three-space manifold *per se* is or not orientable. As shown in [25], the spatial orientability of Minkowski spacetime in itself can be ascertained in principle by the motions of a point electric dipole. Therefore, it is reasonable to expect that the orientability indicator for a dipole can potentially bring about unequivocal information regarding nonorientability of the spatial sections of the spatially flat FRW spacetime. To examine this issue we now turn our attention to topologically induced motions of an electric dipole under quantum vacuum electromagnetic fluctuations.

The spatial components of the four force on a point electric dipole are $f^i = p^j\partial_j E^i$ where $\mathbf{p} = (p^1, p^2, p^3)$ is the electric dipole moment vector. Since the dipole is taken to be a bound system, it is not affected by the expansion of the Universe, which means that the dipole moment $\mathbf{p}$ is a constant vector. Under the same assumptions as made for the point particle, replacing qE^i by $p^j\partial_j E^i$ and following the same steps that led from (7) to (12), the mean squared velocity in each of the three independent directions $i = x, y, z$ is given by

$$\langle\Delta v^i(\mathbf{x},t)^2\rangle = \frac{p^jp^k}{m^2a^2(t)}\int_{t_i}^{t}\int_{t_i}^{t} a^2(t')a^2(t'')\langle(\partial_jE^i(\mathbf{x},t'))(\partial_kE^i(\mathbf{x},t''))\rangle_{\mathrm{FRW}}dt'dt'', \tag{39}$$

which can be conveniently rewritten as

$$\langle\Delta v^i(\mathbf{x},t)^2\rangle = \lim_{\mathbf{x}'\to\mathbf{x}}\frac{p^jp^k}{m^2a^2(t)}\int_{t_i}^{t}\int_{t_i}^{t} a^2(t')a^2(t'')\partial_j\partial'_k\langle E^i(\mathbf{x},t')E^i(\mathbf{x}',t'')\rangle_{\mathrm{FRW}}dt'dt'', \tag{40}$$

where $\partial'_l = \partial/\partial x'_l$ and the summation convention applies only to repeated upper and lower indices.

Now we proceed to the computation of the orientability indicator for a point dipole in spaces E_{17} and E_{16}. The space E_{17} has two topologically special directions: the compact x direction and the flip y direction associated with the nonorientability of E_{17}. To probe the nonorientability of E_{17} by means of stochastic motions it seems most promising to choose a dipole oriented in the y direction, since the orientation of the dipole would also be flipped upon every displacement by the topological length L along the compact direction [25].

For a dipole oriented along the y axis we have $\mathbf{p} = (0, p, 0)$ and

$$\langle \Delta v_x(\mathbf{x}, t)^2 \rangle^{(y)} = \lim_{\mathbf{x}' \to \mathbf{x}} \frac{p^2}{m^2 a^2(t)} \int_{t_i}^{t} \int_{t_i}^{t} a^2(t') a^2(t'') \partial_y \partial_{y'} \langle E_x(\mathbf{x}, t') E_x(\mathbf{x}', t'') \rangle_{\mathrm{FRW}} dt' dt'', \tag{41}$$

where the superscript within parentheses indicates the dipole's orientation. We now proceed as in the case of the charged particle and rewrite the above integral in terms of the conformal time and the correlation function in Minkowski spacetime. It follows that the above equation takes the form

$$\langle \Delta v_x(\mathbf{x}, t)^2 \rangle^{(y)} = \lim_{\mathbf{x}' \to \mathbf{x}} \frac{p^2}{m^2 a^2(t)} \times \int_{\eta_i}^{\eta} \int_{\eta_i}^{\eta} \partial_y \partial_{y'} \langle E_x(\mathbf{x}, \eta') E_x(\mathbf{x}', \eta'') \rangle_M d\eta' d\eta''. \tag{42}$$

Upon replacing the electric-field correlation function by its renormalized version given by Eq. (22), the above equation yields the orientability indicator in the x direction for E_{17}:

$$I^{E_{17}}_{v_x^2}(\mathbf{x}, t)^{(y)}_{\mathrm{FRW}} = \lim_{\mathbf{x}' \to \mathbf{x}} \frac{p^2}{\pi^2 m^2 a^2(t)} \sum_{n_x = -\infty}^{\infty'} \int_{\eta_i}^{\eta} \int_{\eta_i}^{\eta} \partial_y \partial_{y'} \frac{\Delta\eta^2 + r^2 - 2r_x^2}{(\Delta\eta^2 - r^2)^3}, \tag{43}$$

where $\Delta\eta = \eta' - \eta''$, while r_x and r are defined by Eq. (25). Making use of

$$\partial_y \partial_{y'} \frac{\Delta\eta^2 + r^2 - 2r_x^2}{(\Delta\eta^2 - r^2)^3} = -4(-1)^{n_x} \left[\frac{2}{(\Delta\eta^2 - r^2)^3} + 3 \frac{r^2 - r_x^2 + 6r_y^2}{(\Delta\eta^2 - r^2)^4} + 24 \frac{(r^2 - r_x^2) r_y^2}{(\Delta\eta^2 - r^2)^5} \right], \tag{44}$$

we find

$$I^{E_{17}}_{v_x^2}(\mathbf{x}, t)^{(y)}_{\mathrm{FRW}} = -\frac{4p^2}{\pi^2 m^2 a^2(t)} \sum_{n_x = -\infty}^{\infty'} (-1)^{n_x} \{ 2I_1 + 3(r^2 - r_x^2 + 6r_y^2) I_2 + 24(r^2 - r_x^2) r_y^2 I_3 \}, \tag{45}$$

where [25]

$$I_1 = \mathcal{I} = \int_0^{\Delta\eta} \int_0^{\Delta\eta} \frac{d\eta_1 d\eta_2}{[(\eta_2 - \eta_1)^2 - r^2]^3} = \frac{\Delta\eta}{16} \left[\frac{4\Delta\eta}{r^4(\Delta\eta^2 - r^2)} + \frac{3}{r^5} \ln \frac{(r - \Delta\eta)^2}{(r + \Delta\eta)^2} \right], \tag{46}$$

$$I_2 = \int_0^{\Delta\eta} \int_0^{\Delta\eta} \frac{d\eta_1 d\eta_2}{[(\eta_2 - \eta_1)^2 - r^2]^4} = \frac{\Delta\eta}{96} \left[\frac{4\Delta\eta(9r^2 - 7\Delta\eta^2)}{r^6(\Delta\eta^2 - r^2)^2} - \frac{15}{r^7} \ln \frac{(r - \Delta\eta)^2}{(r + \Delta\eta)^2} \right], \tag{47}$$

$$\begin{aligned} I_3 &= \int_0^{\Delta\eta} \int_0^{\Delta\eta} \frac{d\eta_1 d\eta_2}{[(\eta_2 - \eta_1)^2 - r^2]^5} \\ &= \frac{\Delta\eta}{768} \left[\frac{105}{r^9} \ln \frac{(r - \Delta\eta)^2}{(r + \Delta\eta)^2} + \frac{4\Delta\eta(57\Delta\eta^4 - 136r^2\Delta\eta^2 + 87r^4)}{r^8(\Delta\eta^2 - r^2)^3} \right], \end{aligned} \tag{48}$$

in which $\Delta\eta = \eta - \eta_i$.

Similar calculations lead to

$$I^{E_{17}}_{v_y^2}(\mathbf{x},t)^{(y)}_{\mathrm{FRW}} = -\frac{2p^2}{\pi^2 m^2 a^2(t)} \sum_{n_x=-\infty}^{\infty\prime} (-1)^{n_x}\{(5-3(-1)^{n_x})I_1 + 6[r^2+(7-6(-1)^{n_x})r_y^2]I_2 + 48[r^2-(-1)^{n_x}r_y^2]r_y^2 I_3\} \tag{49}$$

and

$$I^{E_{17}}_{v_z^2}(\mathbf{x},t)^{(y)}_{\mathrm{FRW}} = -\frac{4p^2}{\pi^2 m^2 a^2(t)} \sum_{n_x=-\infty}^{\infty\prime} (-1)^{n_x}\{2I_1 + 3(r^2+6r_y^2)I_2 + 24r^2 r_y^2 I_3\}. \tag{50}$$

Since the coincidence limit $\mathbf{x}' \to \mathbf{x}$ has been taken, it follows from Eq. (25) that in Eqs. (45)–(50) one must put

$$r = \sqrt{n_x^2 L^2 + 2(1-(-1)^{n_x})y^2}, \qquad r_x^2 = n_x^2 L^2, \qquad r_y^2 = 2(1-(-1)^{n_x})y^2. \tag{51}$$

For the slab space E_{16} the components of the dipole velocity dispersion are obtained from those for E_{17} by setting $r_x^2 = r^2, r_y = 0$, and replacing $(-1)^{n_x}$ by 1 everywhere. Therefore, we have

$$I^{E_{16}}_{v_x^2}(\mathbf{x},t)^{(y)}_{\mathrm{FRW}} = -\frac{8p^2}{\pi^2 m^2 a^2(t)} \sum_{n_x=-\infty}^{\infty\prime} I_1, \tag{52}$$

$$I^{E_{16}}_{v_y^2}(\mathbf{x},t)^{(y)}_{\mathrm{FRW}} = -\frac{4p^2}{\pi^2 m^2 a^2(t)} \sum_{n_x=-\infty}^{\infty\prime} (I_1 + 3r^2 I_2), \tag{53}$$

$$I^{E_{16}}_{v_z^2}(\mathbf{x},t)^{(y)}_{\mathrm{FRW}} = -\frac{4p^2}{\pi^2 m^2 a^2(t)} \sum_{n_x=-\infty}^{\infty\prime} (2I_1 + 3r^2 I_2), \tag{54}$$

in which $r = |n_x|L$.

It is worth pointing out that the general results obtained for the orientability indicators are independent of a specific gravitation theory, they depend only on the assumption that spacetime is endowed with the spatially flat metric (5). We have also found that the amplitude of the indicator components, both for the charged particle and the electric dipole, is inversely proportional to $a^2(t)$. This was not expected from the outset, and had to be derived.

However, the indicators depend on the scale factor, which is determined by the gravitational theory. Therefore, in order to get definite expressions for the indicators we shall consider a specific model within the framework of general relativity.

VI. A CASE STUDY

The purpose of this section is to study the time evolution of the orientability indicators for spatially flat expanding universes with spatial sections endowed with either of the nontrivial topologies E_{16} or E_{17}. A difficulty arises, however, because the orientability indicators found in the two previous sections, both for the charged particle and the point dipole, are expressed in terms of a mixture of the cosmic time t and the conformal time η, which makes it difficult to bring out their behavior. In order to express the orientability indicators exclusively in terms of t or η one has to know the scale factor as a function of t or η.

As we have mentioned in the Introduction, the metric (5) expresses the principle of spatial homogeneity and isotropy along with the existence of a cosmic time t, with the additional observational input from the Planck collaboration [6,7] that provided strong support for a flat three space ($|\Omega_k| < 0.003$). To study the dynamics of the Universe another assumption is necessary, namely that the large scale structure of the Universe is essentially determined by gravitational interactions, and therefore can be described by a metrical theory of gravity, which we assume to be general relativity.

These very general assumptions constrain the matter content of the Universe to be described by a perfect fluid with energy-momentum tensor

$$T_{\mu\nu} = (\rho + p)u_\mu u_\nu - p g_{\mu\nu}, \tag{55}$$

where u_μ is the fluid four-velocity, ρ is the total energy density, and p is the pressure. In the case of arbitrary space curvature, the Einstein field equations imply the Friedmann equation

$$\frac{\dot{a}^2}{a^2} = \frac{8\pi G}{3}\rho - \frac{k}{a^2}, \tag{56}$$

where G is the gravitational constant. The conservation law $\nabla_\mu T^{\mu\nu} = 0$ leads to the fluid equation

$$\dot{\rho} + 3\frac{\dot{a}}{a}(\rho + p) = 0. \tag{57}$$

Our main interest is to show how valuable the orientability indicators are. Thus, for illustrative purposes we shall consider a model universe that is spatially flat and whose matter content consists of a single-component barotropic perfect fluid with equation of state $p = w\rho$, where the pure number w satisfies $|w| < 1$. In this case the expanding solution to the Friedmann equation (56) with $k = 0$ and the fluid equation (57) is [54]

$$a = \left(\frac{t}{t_0}\right)^{2/(3+3w)}. \tag{58}$$

The age of this Universe is

$$t_0 = \frac{2}{3(1+w)} H_0^{-1}, \tag{59}$$

where H_0 is the Hubble constant, the present value of $H = \dot{a}/a$. According to the latest observational data from the Planck team [7], $H_0 \simeq 67.37\ \mathrm{km/(s\,Mpc)}$ or $H_0^{-1} \simeq 14.5$ Gyr and the age of the Universe is $t_0 \simeq 13.8$ Gyr. In order for Eq. (59) to match these results we choose the equation of state parameter as $w = -0.299$. Thus, from Eq. (58) we find

$$\Delta\eta = \int_{t_i}^{t} \frac{dt'}{a(t')} = \frac{3(1+w)}{1+3w} t_0 \left[\left(\frac{t}{t_0}\right)^{\frac{1+3w}{3(1+w)}} - \left(\frac{t_i}{t_0}\right)^{\frac{1+3w}{3(1+w)}} \right]. \tag{60}$$

By means of this result the orientability indicators found in Secs. IV and V are expressed in terms of the proper time t alone.

It is extremely hard analytically to figure out how the orientability indicators behave as functions of cosmic time because their expressions are given by quite involved infinite sums. The visualization of their behavior can be much more easily accomplished by numerical plots, which is what we shall concentrate on in the following. For all plots we set $t_i = t_0 = 1$, which means that the fluctuations begin to be measured by the orientability indicators at the same reference instant at which the scale factor is unity, that is, today. The compactification length discussed in (2), (3), and Table II is also set equal to unity: $L = 1$. Following [25], the choice $y = 0$, which freezes out the global inhomogeneity degree of freedom, is made in all plots but Fig. 1(a), in which we take $y = 1/2$ to illustrate the global inhomogeneity effect. The orientability indicators are computed from Eqs. (30)–(38) for the charged particle, and Eqs. (45)–(54) for the point dipole, as well as (60) with $w = -0.299$. The infinite sums are rapidly convergent, and the summations are numerically performed taking $n_x \neq 0$ ranging from -50 to 50.

A. Nonorientability: Point charge case

Figure 1 shows orientability indicators as functions of cosmic time for the point charge. In Fig. 1(a) the time evolution of $I^{E_{16}}_{v_x^2}$ given by (37) is shown as a dashed line and that of $I^{E_{17}}_{v_x^2}$, given by (30), is displayed as the dotted line for $y = 0$. These indicators coincide. In Fig. 1(a) we also show as the solid line the indicator $I^{E_{17}}_{v_x^2}$ for $y = 1/2$, exhibiting the global inhomogeneity effect for the E_{17} manifold. In Fig. 1(b), the component of orientability indicator $I^{E_{16}}_{v_y^2}$ given by (38) is represented by a dashed line, whereas the component $I^{E_{17}}_{v_y^2}$, defined by Eq. (31), is depicted as a dotted line. Now these indicator curves are distinct. Thus, it is possible to tell the two topologies apart by means of this component of the indicator. Nevertheless, as will be seen below, the dipole is much more sensitive to nonorientability. The behaviors of the components $I^{E_{17}}_{v_z^2}$ and $I^{E_{16}}_{v_z^2}$ are not shown because the

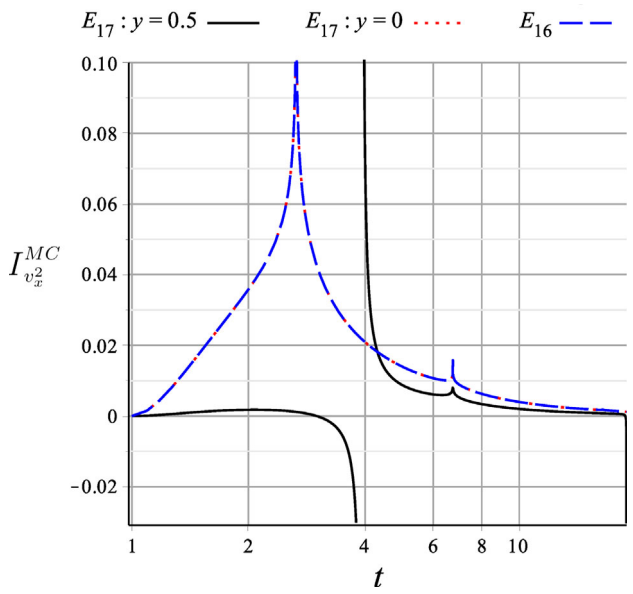

(a)

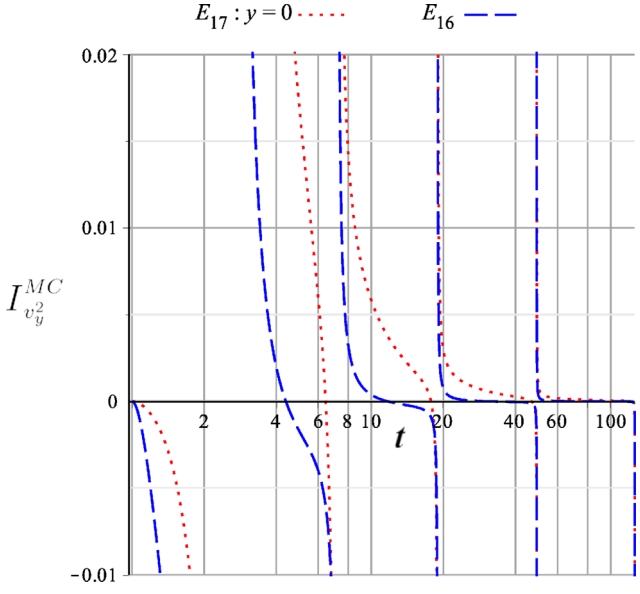

(b)

FIG. 1. Time evolution of orientability indicators for the point charge. In (a) the curve for indicator $I^{E_{17}}_{v_x^2}$ for $y = 0$, shown as a dotted line, coincides with the curve for $I^{E_{16}}_{v_x^2}$, depicted as a dashed line. For $y = 1/2$, the solid curve for $I^{E_{17}}_{v_x^2}$ is now different from the one for $I^{E_{16}}_{v_x^2}$. In (b) the orientability indicators $I^{E_{17}}_{v_y^2}$ and $I^{E_{16}}_{v_y^2}$ are different even for $y = 0$.

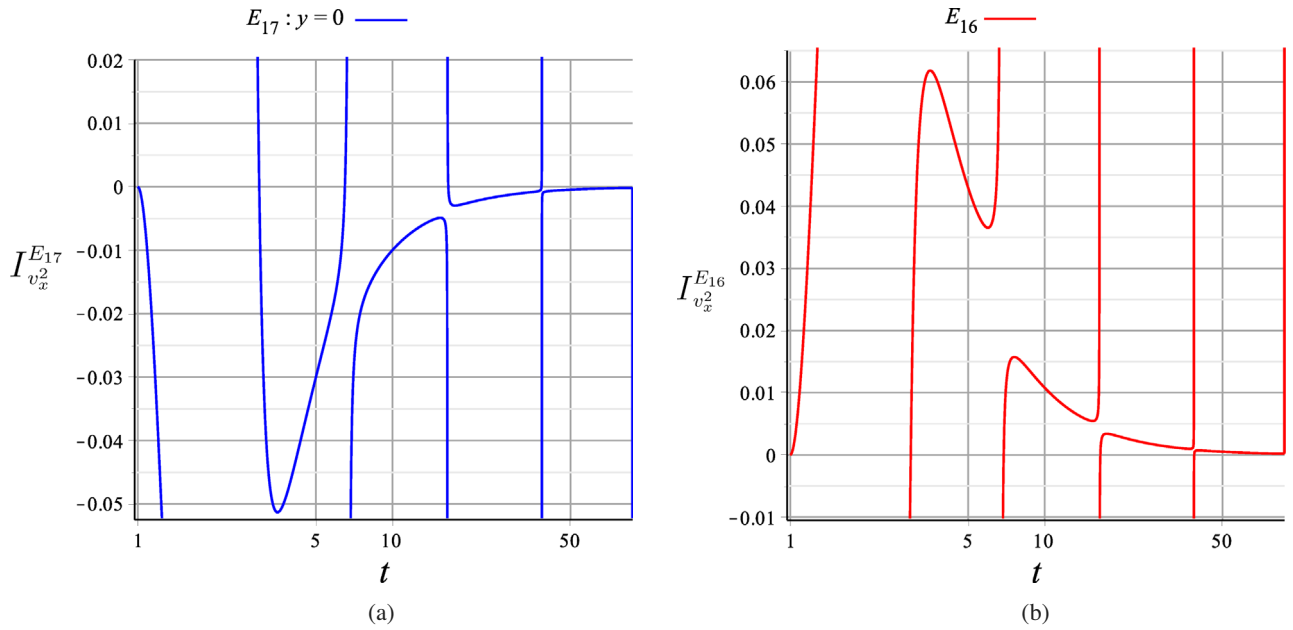

FIG. 2. Under the same conditions as in Fig. 1(b), but now for a point dipole, panel (a) shows the indicator $I^{E_{17}}_{v_x^2}$, whereas panel (b) displays $I^{E_{16}}_{v_x^2}$. We have intentionally made separate plots for the E_{16} and E_{17} topologies to emphasize the repetitious inversion pattern roughly resembling ∪ followed by ∩ in the case of the nonorientable spatial topology. The indicator $I^{E_{16}}_{v_x^2}$ exhibited in panel (b) displays no inversion pattern.

corresponding curves coincide when $y = 0$, as can be directly checked from Eqs. (32) and (38), although they are distinct if $y \neq 0$.

B. Nonorientability: Point dipole case

Figure 2 shows the time evolution of orientability indicators for the point dipole. Figure 2(a) displays the dipole indicator $I^{E_{17}}_{v_x^2}$, given by Eq. (45), and Fig. 2(b) shows $I^{E_{16}}_{v_x^2}$, obtained from Eq. (52). We have intentionally exhibited in separate plots the indicators for the manifolds E_{17} and E_{16} in order to highlight the repetitious pattern roughly resembling ∪ followed by ∩ in the nonorientable case. Similar repetitious inversion patterns are also present in Minkowski spacetime with E_{17} topology [25]. Here the shape of the curves is modified by the dynamical scale factor $a(t)$, though. Just as in the Minkowski case, the orientability indicator is already sensitive to nonorientability even for $y = 0$. The inversion pattern exhibited by E_{17} is qualitatively different from the pattern for E_{16}, which is not characterized by successive inversions, making it possible to identify the nonorientable case in itself.

Figure 3 exhibits the two remaining components of the dipole indicators. Figure 3(a) displays as a dashed line the dipole indicator $I^{E_{17}}_{v_y^2}$ given by (49), together with $I^{E_{16}}_{v_y^2}$, defined by (53), which is depicted as a solid line. Figure 3(b) shows as a dashed line the orientability indicator $I^{E_{17}}_{v_z^2}$ given by (50), as well as $I^{E_{16}}_{v_z^2}$, defined by (54), as a dotted line. Both panels reveal the same inversion pattern roughly resembling successive upward and downward "horns." Similar alternating hornlike inversion patterns emerge in static Minkowski spacetime with E_{17} topology [25]. Now, however, the shape of the curves is modified by the dynamical scale factor $a(t)$. This distinctive pattern allows one to recognize the nonorientability of three-space *per se*.

C. Nonorientabily: Summary of findings

Stochastic motions of a point electric charge under quantum electromagnetic fluctuations give rise to the orientability indicators defined by Eqs. (30)–(38). Figure 1(b) shows that the y component of the orientability indicator for E_{17} is different from the one for E_{16}. Therefore, one can distinguish one topology from the other. But the curve patterns for both topologies are qualitatively the same. This means that the identification of a putative nonorientable topology requires a quantitative comparison of its evolution curves with those for the counterpart orientable topology. In short, we are unable to spot a nonorientable topology *per se* by means of the stochastic motions of a point charged particle.

Things become more appealing when one considers the stochastic motions of a point electric dipole, whose corresponding nonorientability indicators are given by Eqs. (45)–(54). A comparison of the x component of the orientability indicators, exhibited in Fig. 2, already

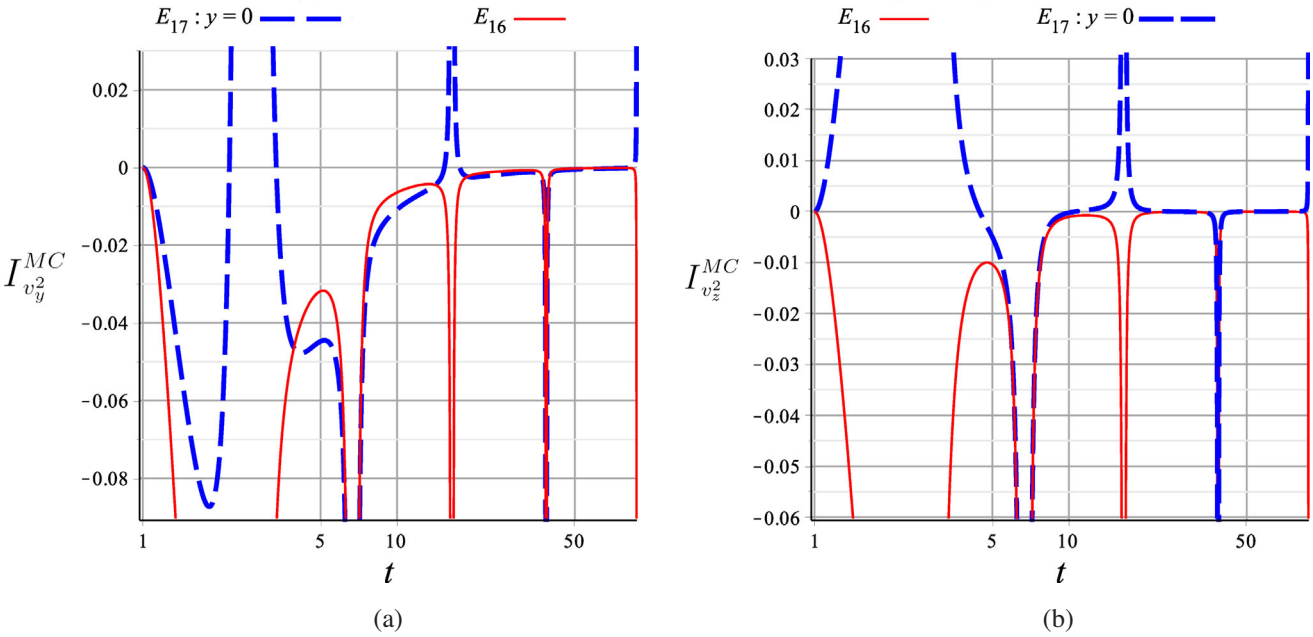

FIG. 3. Under the same conditions as in Fig. 2, and also for a point dipole, panel (a) shows $I^{E_{17}}_{v_y^2}$ as a dashed line and $I^{E_{16}}_{v_y^2}$ as a solid line. Panel (b) displays $I^{E_{17}}_{v_z^2}$ as a dashed line and $I^{E_{16}}_{v_z^2}$ as a solid line. For FRW spacetime with the nonorientable spatial topology, E_{17}, there is an inversion pattern resembling successive upward and downward "horns." Similar alternating hornlike inversion patterns also arise in static Minkowski spacetime with E_{17} topology [25], but here their shape is modified by the dynamical scale factor.

shows a repetitious inversion pattern of roughly resembling ∪ followed by ∩ for E_{17} that distinguishes it from E_{16}. This distinction is much more pronounced when the remaining components of the indicators for E_{17} and E_{16} are compared, as in Fig. 3. The conspicuous pattern roughly resembling alternating upward and downward "horns" for E_{17}, which is absent from the curves for E_{16}, enables us to identify the nonorientability of E_{17} by itself, without the need to compare its indicator curves with those for its orientable counterpart. This is the greatest advantage of the dipole over the point charge in the search for detecting nonorientability through stochastic motions of pointlike objects under quantum vacuum fluctuations of the electromagnetic field.

Contrarily to the dipole case, the point-charge case does not exhibit such prominent qualitative features and hence appears to be of hardly any practical use.

VII. CLOSING REMARKS AND CONCLUSIONS

In the framework of general relativity the Universe is modelled as a four-dimensional differentiable manifold $\mathcal{M}_4$ endowed with the FRW metric (1) that expresses geometrically two basic assumptions of the cosmological modeling, namely the existence of a cosmic time t, which emerges from Weyl's principle, and the cosmological principle, which in turn ensures that the three-dimensional space M_3 is geometrically homogeneous and isotropic. The FRW metric does not specify the topology of the underlying spacetime manifold $\mathcal{M}_4$ or of the corresponding spatial ($t = \text{const}$) sections M_3, which can in principle be found through observations. So far, however, direct searches for a nontrivial topology of M_3 using CMB data from WMAP and Planck have found no convincing evidence of multiple connectedness below the radius of the last scattering surface [6,17–22].[9] In this work, rather than focusing on determining the topology of the spatial sections M_3 of FRW spacetime, we have investigated its global property of orientability.

In the physics at daily and even astrophysical length and time scales we do not find any sign or hint of nonorientability of three space. At the cosmological scale, in order to disclose spatial nonorientability, global trips around the whole three space would be needed to check for orientation-reversing closed paths. Since such global journeys across the Universe are not feasible one might think that spatial orientability cannot be probed. We note, however, that the determination of the spatial topology through, for example, the so-called circles-in-the-sky model, would bring out as a bonus an answer as to three-space orientability at the cosmological scale.

On the other hand, at a theoretical level of reasoning, it is often assumed that the spacetime manifold is separately time and space orientable. As we have mentioned, the arguments supporting orientability combine the space-

[9]This does not exclude the possibility of a FRW universe with a detectable nontrivial cosmic topology [23,55,56].

and-time universality of the local physical laws[10] with a well-defined local arrow of time along with some local results from discrete symmetries in particle physics [28,30]. Of course one is free to resort to such reasonings, but it is reasonable to expect that the ultimate answer to questions regarding the orientability of spacetime should rely on cosmological observations or local experiments, or might come from a fundamental theory of physics.

In this paper we have investigated whether electromagnetic quantum vacuum fluctuations can be used to access the spatial orientability of a FRW expanding spacetime, extending therefore the results of the recent paper [25], where the question of spatial orientability of Minkowski (static) spacetime was examined. To this end, we have studied the stochastic motions of pointlike objects under quantum electromagnetic fluctuations in FRW flat spacetime with the orientable E_{16} (slab) and nonorientable E_{17} (slab with flip) space topologies (cf. Tables I and II).

The statistical indicator $I^{MC}_{v_i^2}$ [Eq. (27)], which measures the departure of the mean square velocity dispersion for pointlike objects in the multiply connected topology from its value for the simply-connected covering space, has been shown to be suitable to reveal spatial orientability of flat FRW spacetime. In the case of a charged particle, we have derived expressions (30)–(38) for the orientability indicator $I^{MC}_{v_i^2}$ for the E_{17} and E_{16} space topologies. Similarly, we have derived expressions (45)–(51) for the indicator (27) corresponding to a point electric dipole oriented in the flip direction of E_{17} topology, and also expressions (52)–(54) for the dipole in three space with the orientable E_{16} topology.

The expressions for the orientability indicators for the particle and the dipole in E_{17} and E_{16} spatial topologies hold for an arbitrary scale factor $a(t)$, which is determined by the gravitational theory. In this way, to concretely study the time evolution of the orientability indicator $I^{MC}_{v_i^2}$ we have assumed in Sec. VI the general relativity theory and also that the matter content consists of a single-component barotropic perfect fluid with equation of state $p = w\rho$, with the equation of state parameter w such that $|w| < 1$. Under these assumptions we have made Figs. 1–3.

Figure 1(a) illustrates the topological inhomogeneity effect of E_{17} topology and makes it clear that $y = 0$ is the appropriate particle's position in E_{17} for comparison of the evolution of the orientability indicator in E_{16} and E_{17} topologies. Figure 1(b) shows that it is possible to distinguish the orientable from the nonorientable topology by comparing the time evolution of the respective y components of the orientability indicator: they give rise to different evolution curves for distinct topologies.

A more ambitious goal is that of finding a way to decide about the orientability of a given spatial manifold in itself, without having to make a comparison of the results for a nonorientable space with those for its orientable counterpart. We have addressed this matter and have shown that the stochastic motions of a point electric dipole can be used to disclose the putative nonorientability of a generic three space *per se*. To this end, under the premises put forward in Sec. VI (flat spacetime in general relativity with perfect fluid source) we have used expressions (43)–(51) and (52)–(54) for the stochastic motions of the dipole in FRW spacetime with, respectively, the nonorientable E_{17} and orientable E_{16} spatial topologies to plot Figs. 2 and 3. These figures show that an inversion pattern for the orientability indicator curves comes about in the case of the nonorientable E_{17} topology, implying that the nonorientability of E_{17} can be detected *per se*.[11]

Our results for the nonorientability indicator hold for any scale factor $a(t)$. For the case studied—flat FRW geometry in the context of general relativity: matter content described by a perfect fluid with equation of state $p = w\rho$ with $w = -0.299$ fixed from the Planck satellite observational data—a nonorientability signature in the form of an inversion pattern was found. All we can be sure of is that there is an inversion pattern in this particular case. In the framework of some other metric gravitational theory or for other scale factors one has to reexamine the question in order to find out whether the scalar factor would preserve, modify, or even destroy the inversion pattern.

An expected result from the beginning of this work was that the role played by the topology on the stochastic motions of particles would depend crucially on the topological compact length L, which in turn gives rise to a lower bound for the timescale required to test orientability. However, the timescale involved in Figs. 1–3 makes it clear that to access the inversion patterns of the orientability indicators one needs a relatively long period of time, typically the time needed to travel across quite a few Ls. A small topological length scale is expected, for example, in the primordial universe. An open question is whether those velocity fluctuations would leave traces that could be extracted from today's observational data, as for example from CMB maps, making it potentially possible to unveil information on three-space orientability. This is a nontrivial and important issue beyond the scope of the present paper, though.

[10]We note that space universality can be looked upon as a topological assumption of global homogeneity of M_3. So, all elements of the covering group Γ are translations, and therefore spatial universality by itself rules out nonorientable three spaces.

[11]The curves for E_{16} display a repetition pattern, which, however is not an inversion pattern.

ACKNOWLEDGMENTS

M. J. Rebouças acknowledges the support of FAPERJ under Grant No. CNE E-26/202.864/2017, and thanks CNPq for the grant under which this work was carried out. We thank C. H. G. Bessa for fruitful discussions. M. J. R. is also grateful to A. F. F. Teixeira for interesting comments, and also for reading the manuscript and indicating typos.

[1] H. Weyl, Z. Phys. **24**, 230 (1923).
[2] H. Weyl, Gen. Relativ. Gravit. **41**, 1661 (2009).
[3] H. P. Robertson, Rev. Mod. Phys. **5**, 62 (1933).
[4] J. V. Narlikar, *Introduction to Cosmology*, 3rd ed. (Cambridge University Press, Cambridge, England, 2002).
[5] S. E. Rugh and H. Zinkernagel, arXiv:1006.5848.
[6] P. A. R. Ade, N. Aghanim, M. Arnaud, M. Ashdown, J. Aumont, C. Baccigalupi, A. J. Banday, R. B. Barreiro, J. G. Bartlett *et al.*, Astron. Astrophys. **594**, A13 (2016).
[7] N. Aghanim, Y. Akrami, M. Ashdown, J. Aumont, C. Baccigalupi, M. Ballardini, A. J. Banday, R. B. Barreiro, N. Bartolo *et al.*, Astron. Astrophys. **641**, A6 (2020).
[8] J. A. Wolf, *Spaces of Constant Curvature* (McGraw-Hill Book Comp., New York, 1967).
[9] W. P. Thurston, *Three-Dimensional Geometry and Topology, Volume 1: Volume 1* (Princeton University Press, Princeton, NJ, 2014).
[10] L. Z. Fang and H. J. Mo, in *Observational Cosmology*, edited by A. Hewitt, G. Burbidge, and L. Z. Fang (D. Reidel Publishing Company, 1987), vol. 124, p. 461, 10.1007/978-94-009-3853-3.
[11] G. F. R. Ellis, Gen. Relativ. Gravit. **2**, 7 (1971).
[12] M. Lachièze-Rey and J. P. Luminet, Phys. Rep. **254**, 135 (1995).
[13] G. D. Starkman, Classical Quantum Gravity **15**, 2529 (1998).
[14] J. Levin, Phys. Rep. **365**, 251 (2002).
[15] M. J. Rebouças and G. I. Gomero, Braz. J. Phys. **34**, 1358 (2004).
[16] J. P. Luminet, Universe **2**, 1 (2016).
[17] P. A. R. Ade, N. Aghanim, C. Armitage-Caplan, M. Arnaud, M. Ashdown, F. Atrio-Barandela, J. Aumont, C. Baccigalupi, A. J. Banday *et al.*, Astron. Astrophys. **571**, A16 (2014).
[18] N. J. Cornish, D. N. Spergel, G. D. Starkman, and E. Komatsu, Phys. Rev. Lett. **92**, 201302 (2004).
[19] J. Shapiro Key, N. J. Cornish, D. N. Spergel, and G. D. Starkman, Phys. Rev. D **75**, 084034 (2007).
[20] P. Bielewicz and A. J. Banday, Mon. Not. R. Astron. Soc. **412**, 2104 (2011).
[21] P. M. Vaudrevange, G. D. Starkman, N. J. Cornish, and D. N. Spergel, Phys. Rev. D **86**, 083526 (2012).
[22] R. Aurich and S. Lustig, Mon. Not. R. Astron. Soc. **433**, 2517 (2013).
[23] G. I. Gomero, B. Mota, and M. J. Rebouças, Phys. Rev. D **94**, 043501 (2016).
[24] C. H. G. Bessa and M. J. Rebouças, Classical Quantum Gravity **37**, 125006 (2020).
[25] N. A. Lemos and M. J. Rebouças, Eur. Phys. J. C **81**, 618 (2021).
[26] A. Matas, D. Müller, and G. Starkman, Phys. Rev. D **92**, 026005 (2015).
[27] Y. B. Zel'dovich and I. D. Novikov, Sov. J. Exp. Theor. Phys. Lett. **6**, 236 (1967).
[28] S. W. Hawking and G. F. R. Ellis, *The Large Scale Structure of Space-Time*, Cambridge Monographs on Mathematical Physics (Cambridge University Press, Cambridge, England, 2011).
[29] R. Penrose and W. Rindler, *Spinors and Space-time, Volume 1, Two-Spinor Calculus and Relativistic Fields* (Cambridge University Press, Cambridge, England, 1986).
[30] R. Geroch and G. T. Horowitz, in *General Relativity: An Einstein Centenary Survey*, edited by S. W. Hawking and W. Israel (Cambridge University Press, Cambridge, 1979), pp. 212–293.
[31] M. J. Hadley, Classical Quantum Gravity **19**, 4565 (2002).
[32] M. Hadley, Preprints **2018**, 2018040240 (2018).
[33] R. P. Geroch, J. Math. Phys. (N.Y.) **9**, 1739 (1968).
[34] R. P. Geroch, J. Math. Phys. (N.Y.) **11**, 343 (1970).
[35] J. R. Weeks, *The Shape of Space*, 3rd ed. (CRC Press, Boca Raton, 2020).
[36] S. Weinberg, *Gravitation and Cosmology: Principles and Applications of the General Theory of Relativity* (John Wiley and Sons, New York, 1972).
[37] C. H. G. Bessa, V. B. Bezerra, and L. H. Ford, J. Math. Phys. (N.Y.) **50**, 062501 (2009).
[38] H. Yu and L. H. Ford, Phys. Rev. D **70**, 065009 (2004).
[39] R. M. Wald, *General Relativity* (Chicago University Press, Chicago, USA, 1984).
[40] N. D. Birrell and P. C. W. Davies, *Quantum Fields in Curved Space*, Cambridge Monographs on Mathematical Physics (Cambridge University Press, Cambridge, England, 1984).
[41] A. Riazuelo, J. Weeks, J. P. Uzan, R. Lehoucq, and J. P. Luminet, Phys. Rev. D **69**, 103518 (2004).
[42] H. Fujii and Y. Yoshii, Astron. Astrophys. **529**, A121 (2011).
[43] C. Jun and Y. Hong-Wei, Chin. Phys. Lett. **21**, 2362 (2004).
[44] L. H. Ford, Int. J. Theor. Phys. **44**, 1753 (2005).
[45] H. Yu, J. Chen, and P. Wu, J. High Energy Phys. 02 (2006) 058.
[46] M. Seriu and C. H. Wu, Phys. Rev. A **77**, 022107 (2008).
[47] V. Parkinson and L. H. Ford, Phys. Rev. A **84**, 062102 (2011).
[48] V. A. De Lorenci, C. C. H. Ribeiro, and M. M. Silva, Phys. Rev. D **94**, 105017 (2016).
[49] H. Yu, Phys. Rev. D **70**, 125006 (2004).

[50] R. Lehoucq, M. Lachieze-Rey, and J. P. Luminet, Astron. Astrophys. **313**, 339 (1996).
[51] G. I. Gomero, M. J. Rebouças, and R. K. Tavakol, Classical Quantum Gravity **18**, 4461 (2001).
[52] G. I. Gomero, A. F. F. Teixeira, M. J. Rebouças, and A. Bernui, Int. J. Mod. Phys. D **11**, 869 (2002).
[53] M. J. Rebouças, Int. J. Mod. Phys. D **09**, 561 (2000).
[54] B. Ryden, *Introduction to Cosmology* (Addison-Wesley, San Francisco, 2002).
[55] A. Bernui, C. P. Novaes, T. S. Pereira, and G. D. Starkman, arXiv:1809.05924.
[56] R. Aurich, T. Buchert, M. J. France, and F. Steiner, Classical Quantum Gravity **38**, 225005 (2021).